

Influence of Sulfur on Heterogeneous Nucleus of Spheroidal Graphite

Hideo Nakae¹ and Yoshio Igarashi²

¹Laboratory for Materials Science and Technology, Waseda University, Tokyo 169-8555, Japan

²Casting Technology Research Lab., Hitachi Metals, Ltd., Mooka 321-4367, Japan

The nuclei of spheroidal graphite (abbreviated SG) were studied using an FE-SEM and an EDS. Many kinds of SG irons with different sulfur contents were prepared for the observation of the nucleus-like core materials. The Mg-treated SG iron was cast into a thin CO₂ sand mold and a chilled test piece that is usually used for chemical analysis. The core materials were observed using the chilled test piece. The number of SGs is maximum in the range from 0.010 to 0.025 mass%S of the base melt and the nucleus material is MgS. We propose that this is the most desirable S content for the production of the SG iron castings. This S level is nearly identical to that of the base melt chemical composition for commercial SG iron production. If the S content of the base melt is greater than 0.005 mass%S, the SG nucleus is a spherical MgS in the Mg-treated SG iron. On the other hand, when the S content is less than 0.0022 mass%, the nucleus is a hexagonal (Mg, Si, Al)N as reported by Skaland and Solberg *et al.*

(Received June 26, 2002; Accepted September 4, 2002)

Keywords: nucleation of spheroidal graphite, heterogeneous nucleus, graphite nodule number, activity of sulfur, microanalysis

1. Introduction

After the invention of spheroidal graphite (abbreviated SG) iron treated with Ce by Morrogh and Williams^{1,2)} and treated with Mg by Gagnebin *et al.*,³⁾ many research studies^{4,5)} have been done in order to explain the spheroidizing mechanism. Many overview papers have also been published such as that by Lux.⁴⁾ There are of course the nucleation theories for SG formation.^{6,7)} Nevertheless, the mechanism has still not been totally clarified.

We have already summarized the characteristics of the nucleus of SG for many kinds of SG irons based on a field emission-type scanning electron microscope (abbreviated FE-SEM) observations.⁶⁻⁹⁾ We described the effect of S on the graphite nodule number, and this number has a maximum at 0.010–0.025 mass%S.⁸⁾ Therefore, in this paper, we discuss the influence of the S content on the nucleus materials of SG due to the observed results for the SG iron.

There are many reports that have described the heterogeneous nuclei of SGs such as that by Rosenstiel¹⁰⁾ and also that by Igarashi.^{11,12)} Igarashi recently described the heterogeneous nuclei of SG using an FE-SEM, a field emission-type Auger electron spectroscopy and a transmission electron microscope. Horie¹³⁾ was interested in the nucleation effect of rare earth elements (abbreviated RE) and summarized that the sulfide acts as a nucleus for SG. Identical phenomena were also recognized by Lalich.¹⁴⁾ However, Skaland¹⁵⁾ recently reported that the hexagonal nuclei are composed of double layer materials, namely a MgS and CaS core surrounded by MgO·SiO₂ and 2MgO·SiO₂. They proposed an epitaxial growth mechanism of graphite on the oxide. There is a big disagreement between these results and Skaland's result for the nucleus materials. We think the main reason is as follows. Skaland¹⁵⁾ used the base melt with a very low S level, such as 0.0036 mass%S calculated using the chemical composition of their raw materials. Moreover, Solberg¹⁶⁾ studied the structure and composition of the hexagonal nuclei of the SGs and reported during the past year that the nuclei are suggested to

be AlMg_{2.5}Si_{2.5}N₆.

Considering these results, we studied the influence of S on the nucleus materials of the Mg-treated SG iron for different S content melts. We then observed the heterogeneous nucleus of the SGs for many kinds of iron base melts that differed in S content using an FE-SEM.

2. Experimental Procedure

2.1 Sample preparation

We prepared many kinds of SG iron samples with different S levels.⁸⁾ The S content of the base melts was changed from 0.0004 to 0.084 mass%S. These samples were made of pure iron, electrolytic iron and high purity electrolytic iron, which were selected by the targeted S levels, and electrode graphite, ferro-silicon, ferro-manganese and ferro-sulfur. The SG iron was spheroidized with a Fe–50 mass%Si–6 mass%Mg alloy that contained a small amount of Ca, RE, Al and Ba. The melt was inoculated before casting. The chemical composition of the spheroidizer and the inoculant are shown in Table 1.

The magnesium treatment was carried out at the 0.5 mass%, 0.9 mass% and 1.3 mass% addition of the spheroidizer, namely, the amounts of Mg addition were 0.029 mass%, 0.053 mass% and 0.076 mass% respectively. The melt was inoculated with 0.3 mass% of the ferro-silicon. The melt was then cast into a thin 2.0 mm thick plate in a CO₂-sand mold for the counting of the SG numbers. The cooling rate was from 16 K/s to 25 K/s just after the solidification. The melt was also cast into rapidly cooled chill samples, as conventionally used for atomic emission spectral analysis, for the observation of the SG nucleus to obtain fine SG for better ob-

Table 1 Chemical composition of spheroidizer and inoculant. (mass%)

	Si	Mg	Ca	Ce	La	Ba	Al	Fe
Spheroidizer	46.8	5.9	2.0	0.5	0.4	0.04	0.5	balance
Inoculant	69.3	—	1.8	—	—	0.03	2.0	—

servation of the nucleus.

2.2 Observation of nucleus materials

The method of sample preparation was identical to that in previous reports.^{11,12)} To achieve a high probability of obtaining a section passing near the center of an SG, we selected fine SGs. Strict attention was paid to preserving the fracture of the internal structure of graphite during specimen preparation. The specimens were mechanically polished using diamond paste and then subjected to argon ion etching. The preparation steps for the specimens are shown in Fig. 1. The observation of the SG nucleus was done using an FE-SEM and an energy dispersive X-ray spectrometer (EDS) attached to the FE-SEM.

3. Results and Discussion

3.1 Diameter of SGs and the nodule count

The chemical composition of the Mg-treated iron is shown in Table 2. The chemical composition is nearly identical to that of the commercial SG iron except for the impurity elements.

The microstructures of these samples, treated with 0.076 mass%Mg, are shown in Fig. 2. The matrix of the 0.00035 mass%S sample cooled at 25 K/s is mainly ledeburite and there is small number of SGs. The matrix of the others are ferrite and pearlite. The graphite morphology of the 0.084 mass%S sample is flake and the others are spheroidal.

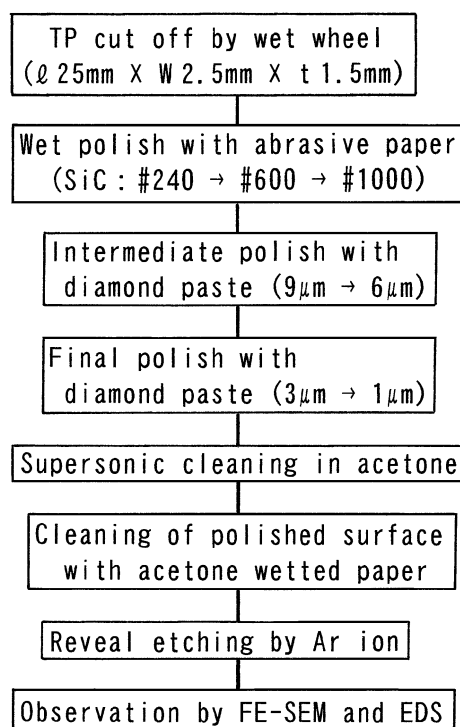


Fig. 1 Procedure of sample preparation for FE-SEM observation.

Table 2 Chemical composition of Mg-treated iron. (mass%)

C	Si	Mn	P	S	Cu	Mg	Cr
3.60	2.10	0.33		0.0004		0.018	
~3.80	~2.40	~0.39	<0.01	~0.059	<0.02	~0.045	<0.02

The number of SGs in the thin plate castings, N_A mm⁻², is shown in Fig. 3 as a function of the amount of Mg addition, cooling rate and the S levels of the base melts.⁸⁾ The peak changes with the S levels and the Mg addition. The relationship between N_A and the S content of the base melt shows a peak at the S level from 0.010 to 0.025 mass%S. As is well known, the formation of cementite can be depressed by the large SG number, N_A , for the production of a thin SG iron casting. Moreover, the formation of chunky graphite in a heavy SG castings should be controlled by the N_A , because the graphite number determines the thickness of the austenite layer during the eutectic solidification¹⁷⁾ and the shrinkage tendency of the SG iron castings is also controlled by N_A .¹⁸⁾ Therefore, the SG number is the most important factor for the production of sound SG iron castings.

3.2 Nucleus-like materials of SG

The matrix structure of the Mg-treated iron, in the high purity base melt (0.00035 mass%S) solidifies to ledeburite and a small number of SGs, as shown in Fig. 2. Therefore, it is very difficult to find an SG in the rapidly cooled chill sample. We then observed the nucleus materials of the SGs which contain more than 0.0022 mass%S.

The nucleus-like core materials of the Mg-treated 0.0022 mass%S sample are shown in Fig. 4. They are the typical examples of the highly magnified structure of rectangular, pentagonal and hexagonal nucleus-like cores; the diameters are about 1 μm, consisting of (Mg, Si, Al)N along with (Ca, Mg)S and MgO. The shape of the core is mainly rectangular along a small number of spherical ones which are MgO or (Ca, Mg)S.

The Mg-treated 0.0052 mass%S sample is shown in Fig. 5. There are many spherical nucleus-like cores with diameters of about 1 μm consisting of MgS along with MgO, (Mg, Si, Al)N as shown in Fig. 5(b).

The microstructures of the SG of the 0.013 mass%S sample are shown in Fig. 6. There are spherical MgS nuclei with a diameter of about 1 μm, accompanied by MgO, (La, Ce, Nd)S and (Mg, Si, Al)ON. If the base melt contains more than 0.050 mass%S, the large spherical MgS is dominant and the diameter is more than 1 μm as shown in Fig. 6.

Figures 7(a) and (b) show that there is a large nucleus-like core of MgS in the SG and a small spherical MgS outside of the SG in the 0.072 mass%S sample. As can be clearly seen, the large MgS acts as a nucleus for the graphite. However, the small one does not act as a nucleus due to the curvature effect. If the size is nearly identical, as shown in Fig. 6(c), both act as a nucleus.

As already described, if the base melt contains 0.084 mass%S, the Mg-treated iron solidifies to flake graphite. In this case, the spherical MgS acts as a nucleus for the flake graphite as shown in Fig. 8(a), nevertheless, it does not act as the nucleus of SG. These results show that the identical material acts as a nucleus for SG and flake graphite. What does this mean? We support the interfacial energy theory^{19,20)} as the SG formation mechanism. It is well known that the nucleation potential is a function of the lattice registry parameter,²¹⁾ however, it is very difficult to imagine the formation of spheroidal graphite based on the nucleation theory. For example, the SG formation observations

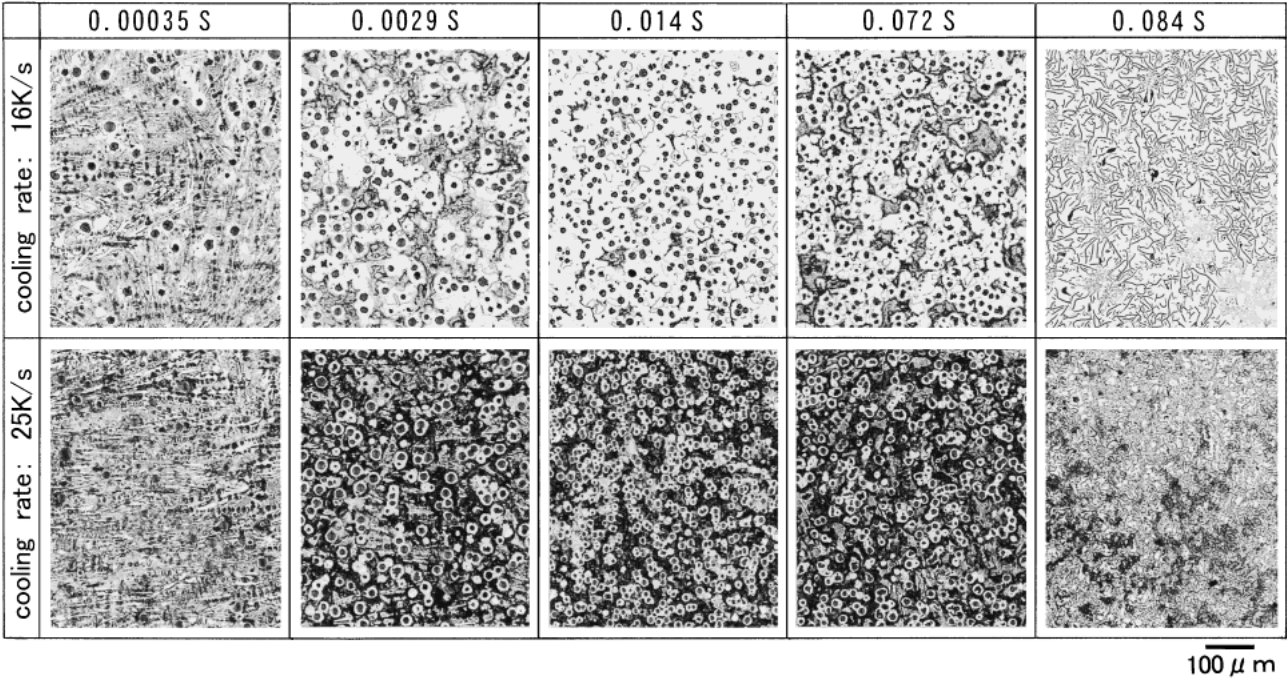


Fig. 2 Optical microstructure of graphite for these samples.

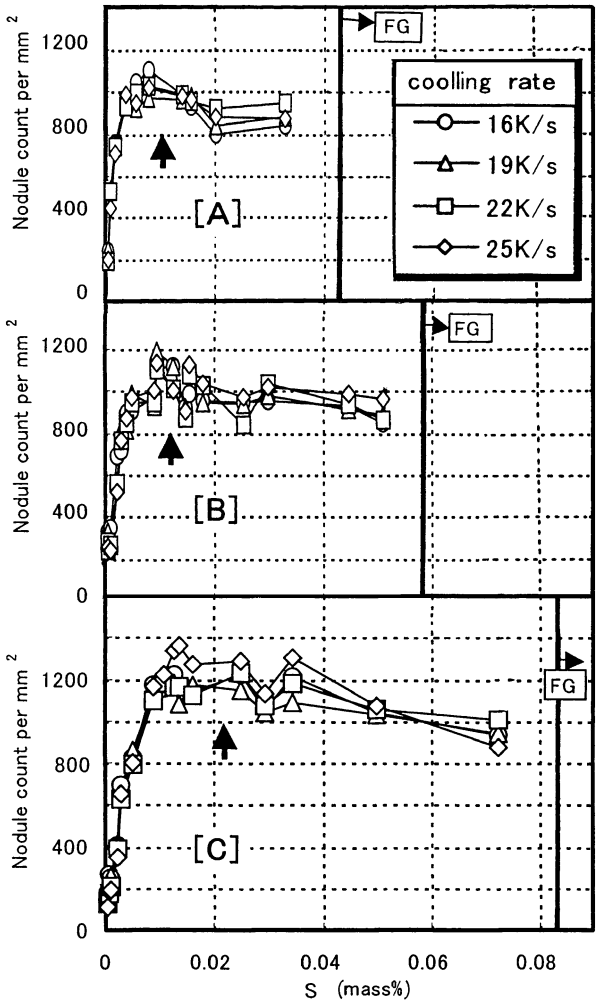


Fig. 3 Influence of S content of base melt and the addition of Mg on number of SG iron cast in 2 mm thin plate. Mg addition, [A]: 0.029 mass%, [B]: 0.053 mass% and [C]: 0.076 mass%.

by Igarashi^{11,12)} and Horie¹³⁾ showed that the morphology of the initial graphite is not spherical and grows into a spherical shape later. This means that the growth mode determines the graphite shape.

We summarized the observed results for the nucleus core materials based on the influence of the S content in the base melt in Table 3. These results clarified that the nucleus material of the 0.0022 mass%S base melt is mainly rectangular (Mg, Si, Al)N and the size is 0.5–1.0 μm. This result is nearly identical with the result of Skaland¹⁵⁾ except for oxygen. When S in the base melt is more than 0.0052 mass%, the nucleus materials consist of spherical MgS. As already described, Skaland *et al.* used a very low S level base melt, such as 0.0036 mass%S. Therefore, we consider that the S levels in the base melts is the main reason for the significant discrepancy with us in the nucleus materials of the SGs. Moreover, our results show that the optimum S content in the base melt is from 0.010 to 0.025 mass% for the nucleation of the SGs and the nucleus-like core material is spherical MgS. These S levels agree with that of the commercial SG iron production.

Table 4 shows the summarized information on the nucleus-like core materials based on our previous results.⁷⁾ If we consider that the nucleus of SG is based on Tables 3 and 4, not only the nucleus-like core materials, but also the diameter and the shape differ from production process to production process. The chemical compositions of these nuclei have nothing in common. Nevertheless, the shape of the nucleus-like core is mainly spherical. What does this mean? The spherical shape implies that the cores should be in a liquid state or be vitreous at the time of SG formation.¹¹⁾ We think that this phenomenon is identical with the nucleation effect of Bi on SG.²²⁾ The lattice parameter of the nucleus should be considered if the core is crystalline. Nevertheless, the core must be liquid or vitreous during the time of the SG formation, so that the crystal lattice matching cannot be considered in this

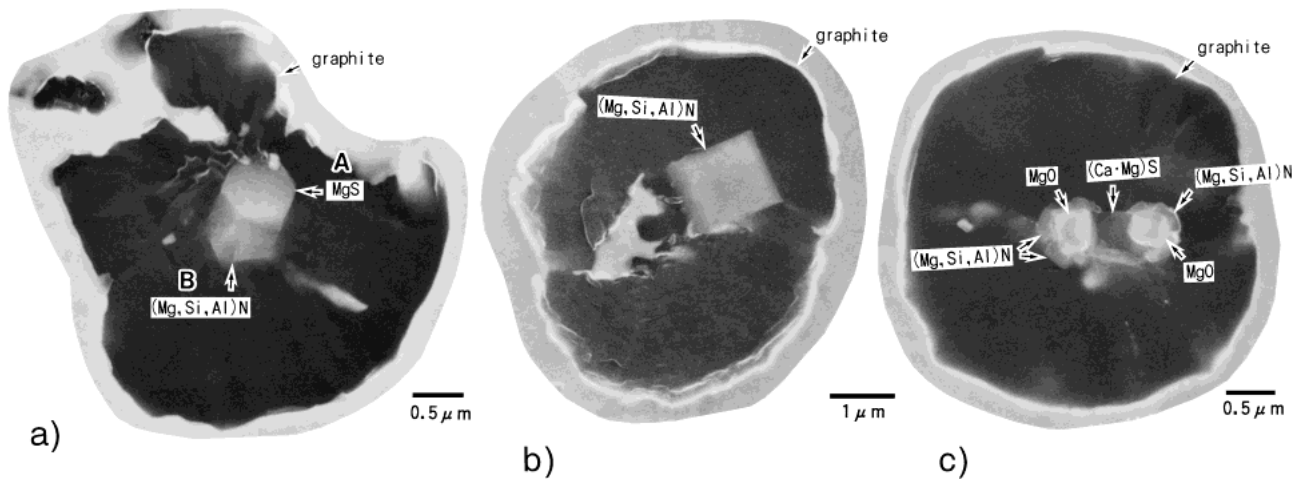


Fig. 4 SEM observation of graphite nucleus-like cores in Mg-treated iron for 0.0022 mass% S base melt.

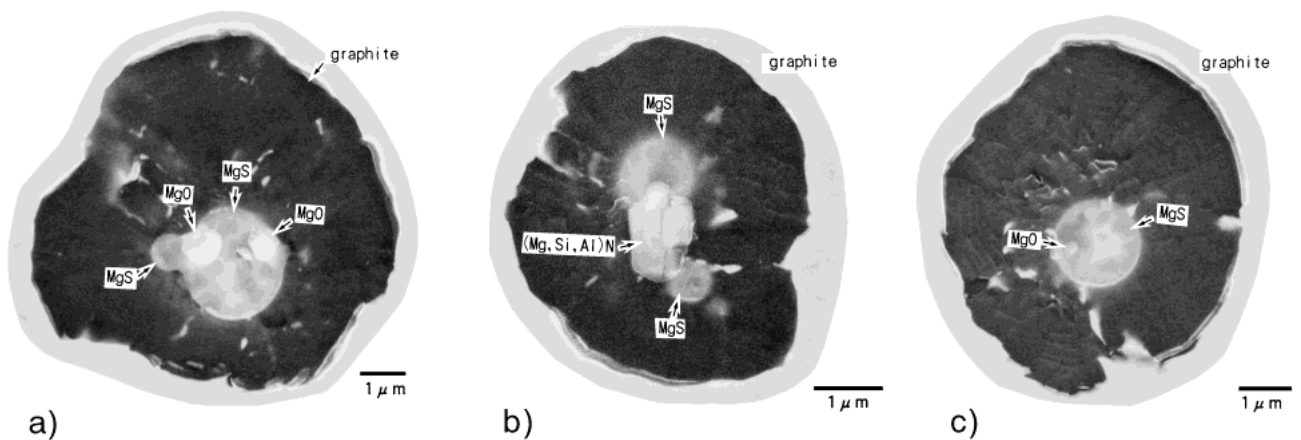


Fig. 5 SEM observation of graphite nucleus-like cores in Mg-treated iron for 0.0052 mass% S base melt.

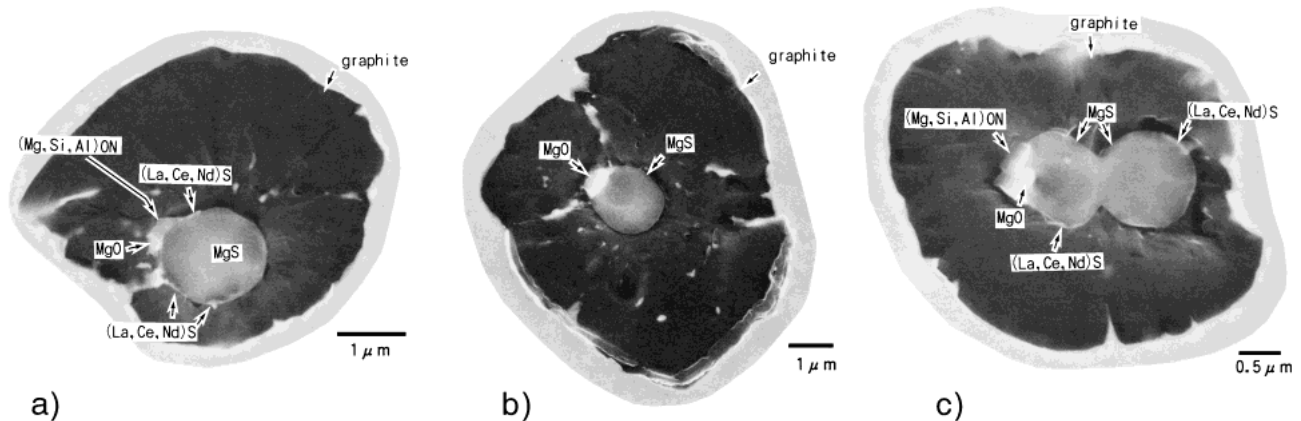


Fig. 6 SEM observation of graphite nucleus-like cores in Mg-treated iron for 0.013 mass% S base melt.

paper.

The shape of a crystallized sulfide, such as MgS, should be polygonal. We already reported the shape of the nucleus cores for the commercial grade Mg-treated iron cast into the chilled samples as polygonal and spherical MgSs coexist as already reported.⁷⁾ Nevertheless, we cannot confirm the formation of graphite on the polygonal shapes. All of the graphite crystallizes on the spherical MgSs.⁷⁾ This means that the vitreous core is superior in nucleation effect to that of the crystallized

one. Therefore, we now believe that this result agrees with the nucleation effect of Bi on SG,²²⁾ in which the Bi should be liquid at the SG formation temperature.

If a fine liquid droplet is not wetted by the iron melt, the droplet/melt interphase acts as a space for the nucleation site of graphite because the atomic radius of C is very small. Therefore, C can be diffused and crystallized at the interphase as a nucleus site for graphite. This mechanism is identical with the bubble theory,²³⁾ in which graphite can crystallize or

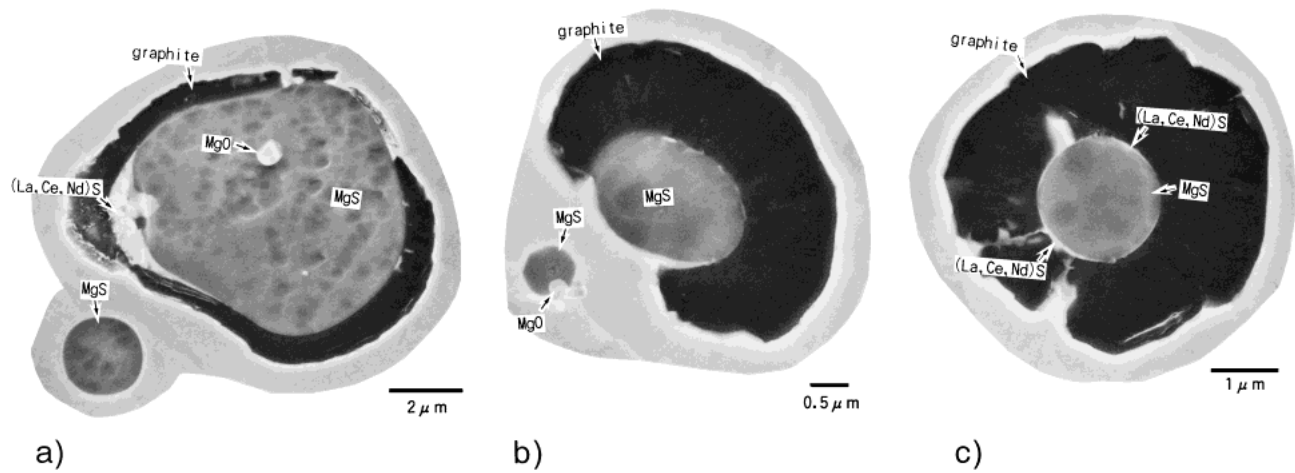


Fig. 7 SEM observation of graphite nucleus-like cores in Mg-treated iron for 0.072 mass% S base melt.

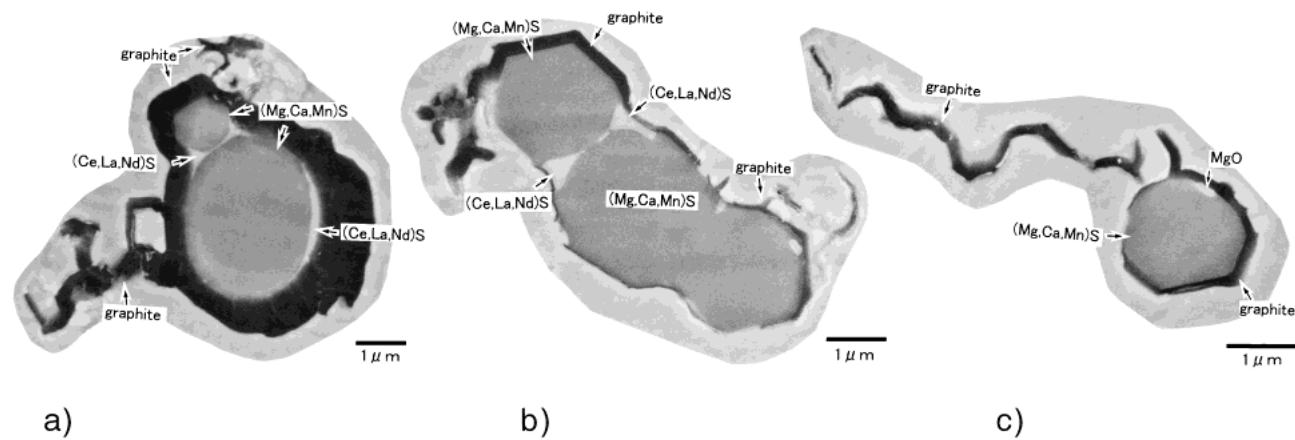


Fig. 8 SEM observation of graphite nucleus-like cores in Mg-treated iron for 0.084 mass% S base melt.

Table 3 Influence of base metal S content on nucleus materials of SGs for Mg treated iron.

mass% S of BM*	Nucleus materials			
	shape of N**	dia. (μm)	NM***	OM****
0.0022	rectangle	0.5–1.0	(Mg, Si, Al)N	MgS, MgO, (Ca·Mg)S
0.0052	spherical	//	(Mg, Ca)S	MgO, (Mg, Si, Al)N
0.013	//	//	(Mg, Ca)S	MgO, (Mg, Si, Al)ON, (La, Ce, Nd)S
0.050	//	1.0–2.0	(Mg, Ca)S	MgO, (La, Ce, Nd)S
0.072	//	1.5–5.0	(Mg, Ca)S	MgO, (La, Ce, Nd)S
0.083	// / faceted	1.5–5.0	(Mg, Ca, Mn)S	MgO, (La, Ce, Nd)S

* base melt, ** nucleus, *** nucleus materials, **** other materials

precipitate at the liquid/vapor interphase.^{13,23)} These results show that the formation of SG is not based on the nucleus materials, namely, the epitaxial growth, but on the condition of the graphite growth mode to form spheroids. There is only one common factor, that is, the low activities of S and O.

We theorize that the addition of a spheroidizing element, such as Mg, Ca, Ce *etc.* is not theoretically needed for the production of the SG iron. They act to decrease the activity of S and O in the melt as Sabramanian reported²⁴⁾ which described the formation range of the activity of S, which is

less than 0.03, and the activity of O which is less than 10^{−7}. The critical activity value of S for the SG formation is identical with the critical S activity value where the onset of the decrease in the surface tension of the carbon-saturated iron melt occurs, as reported by Keverian.²⁵⁾ Therefore, the Fe–C melted in a He–3 vol% H₂ atmosphere and the Fe–C–Si iron melted in a vacuum easily to form SG due to the low activity of S and O.⁷⁾ Based on these results we support the interfacial energy theory for the formation mechanism of SG.

Many kinds of materials can be the nucleus of SG as al-

Table 4 Influence of treatment process on nucleus materials of SGs.

Samples	Shape of N*	dia. (μm)	NM**	OM***
Mg treated	spherical	0.5–1.0	MgS or (Mg-Si-Al)N	MgO + (Mg-Si-Al)N
RE treated	spherical	0.5–1.0	RES	(Ce-La-Nd) O_xS_y
Ca treated	spherical	0.2–0.5	CaS or (Al-Mg-Si)N	MgO·Al ₂ O ₃
Pure Fe–C	agglomerated	0.2–0.5	FeCl _x	(Mg·Al·Si)O
Pure Fe–C–RE	spherical	0.5–1.0	RES	
Pure Fe–C–Si	spherical	0.1–0.2	SiO ₂	

* shape of nucleus, ** nucleus materials, *** other materials

ready described for the low activity melt of S and O. Nowadays, we can easily produce SG iron castings by the addition of a spheroidizer, nevertheless, we cannot significantly increase the nodule number. If the SG number increases, the formation of ledeburite, the shrinkage cavity and chunky graphite can be depressed.^{17,18,26)} Therefore, one of the most important subjects for the SG iron casting production is how to increase the number of SGs. Therefore, we propose controlling the S content in the base melt in order to form the spherical MgSs as the nucleation site of the SGs.

4. Conclusions

The SG nuclei were studied using an FE-SEM and an EDS. Many kinds of Mg-treated SG irons with different sulfur contents were prepared for observation of the nucleus-like core materials. The SG irons were cast into a thin CO₂ sand mold with a 2 mm thickness in order to count the SG nodule number and into a chilled chemical analysis test piece for observation of the nucleus. The results are as follows:

(1) The peaks of the SG number is a maximum for the sulfur content of base melt, from 0.010 to 0.025 mass%, and is also affected by the amount of Mg addition.

(2) The range from 0.010 to 0.025 mass%S is the most desirable S content for the production of the SG iron castings in order to increase the SG nodule number. This S level is nearly identical with that of the chemical composition of the base melt for commercial SG iron production.

(3) If the S content of the base melt is greater than 0.005 mass%S, the nucleus of SG is mainly spherical MgS. On the other hand, when the S content is less than 0.0022 mass%, the nucleus is rectangular (Mg, Si, Al)N.

(4) The chemical composition of the nucleus materials of Mg-treated SG is changed by the S content of base melt from rectangular (Mg, Si, Al)N to spherical MgS. Therefore, the spherical MgS is the most suitable nucleus materials for the Mg-treated SG iron.

REFERENCES

- 1) H. Morrogh and W. J. Williams: J. Iron and Steel Inst. **155** (1947) 321–371.
- 2) H. Morrogh and W. J. Williams: J. Iron and Steel Inst. **156** (1948) 306–322.
- 3) A. P. Gagnebin, K. D. Millis and N. B. Pilling: The Iron Age **17** (1949, 2) 77–84.
- 4) B. Lux: AFS Cast Metals Res. J. (1972, 3) 25–38.
- 5) The Metallurgy of Cast Iron: B. Lux, I. Minkoff and F. Mollard Co-eds, Georgi Publishing Co. (1975).
- 6) R. J. Warrick: AFS Trans. **74** (1966) 722–733.
- 7) H. Nakae, Y. Igarashi and Y. Ono: J. Jap. Foundry Eng. Soc. **73** (2001) 111–117.
- 8) Y. Igarashi and H. Nakae: J. Jap. Foundry Eng. Soc. **74** (2002) 30–35.
- 9) Y. Igarashi and S. Okada: Hitachi Metals Tech. Rev. **13** (1997) 65–70.
- 10) A. P. von Rosenstiel and H. Bakkerus: Giesserei Tech-Wiss. Beihefte **16** (1964) 149–154.
- 11) Y. Igarashi and S. Okada: Int. J. Cast Metals Res. **11** (1998) 83–88.
- 12) Y. Igarashi and S. Okada: J. Jap. Foundry Eng. Soc. **71** (1999) 745–751.
- 13) H. Horie, T. Kowata, K. Abe and A. Chida: J. Jap. Foundry Eng. Soc. **57** (1985) 778–783.
- 14) M. J. Lulich and J. R. Hichings: AFS Trans. (1976) 653–664.
- 15) T. Skaland, Ø. Grong and T. Grong: Metall. Trans. **24A** (1993) 2321–2345.
- 16) J. K. Solberg and M. I. Onsjøen: Mater. Sci. Tech. **17** (2001) 1238–1242.
- 17) H. Nakae and H. Shin: Proc. SCAI (2001) 336–343.
- 18) H. Nakae and T. Kanno: Proc. 7th AFC (2001) 109–117.
- 19) J. Keverian, H. F. Taylor and J. Wulff: American Foundryman (1953,6) 85–91.
- 20) G. T. van Rooyen and G. Paul: Met. Sci. **8** (1974) 370–382.
- 21) B. L. Bramfitt: Trans. **1** (1970) 1987–1995.
- 22) H. Horie and T. Kowata: J. Jap. Foundry Eng. Soc. **60** (1988) 173–178.
- 23) S. I. Karsay: *Recent Research on Cast Iron*, H. Merchant Ed. Gordon and Breach (1968) 215–239.
- 24) S. V. Sabramanian, D. A. R. Kay and G. R. Purdy: *The Physical Metallurgy of Cast Iron*, (North-Holland, 1985) 47–56.
- 25) J. Keverian and H. F. Taylor: Trans. AFS **65** (1957) 212–221.
- 26) H. Nakae and Y. Igarashi: J. Jap. Foundry Eng. Soc. **74** (2002) 197–204.